Aust. J. Phys., 1998, **51**, 903–11

Cross Section Measurements of Two-nucleon Pickup Reactions in the ^{13}C+d System at Deuteron Energies below 350 keV

A. A. Naqvi,[A] *M. M. Nagadi,*[A] *S. Kidwai,*[B]
M. A. Al-Ohali[A] *and F. Z. Khiari*[A]

[A] Center for Applied Physical Sciences,
King Fahd University of Petroleum and Minerals,
Dhahran, Saudi Arabia.
[B] Department of Physics, King Fahd University of Petroleum and Minerals,
Dhahran, Saudi Arabia.

Abstract

Cross sections of two-nucleon pickup reactions in the ^{13}C+d system, i.e. ^{13}C(d, α_0)^{11}B and ^{13}C(d, α_1)^{11}B* reactions have been measured for 180–350 keV deuterons. The angular distributions were measured in steps of 20 keV at 14 angles ranging from 30° to 164°, while the excitation functions were measured at 90° in steps of 10 keV. The excitation functions of ^{13}C(d, α_0)^{11}B and ^{13}C(d, α_1)^{11}B* reactions with 5·167 and 3·307 MeV Q-values, respectively, exhibit smooth variations of cross section with energy. The angular distribution of ^{13}C(d, α_0)^{11}B reaction is asymmetric. With decreasing deuteron energy, the degree of asymmetry increases and below 220 keV deuteron energy the angular distribution is backward-peaked. This indicates a dominating contribution from the direct reaction in this channel below 220 keV deuteron energy. The angular distribution of ^{13}C(d, α_1)^{11}B* reactions are highly symmetric about 90°, indicating a dominating compound nucleus contribution over this energy range. The trends of angular distribution of ^{13}C(d, α_0)^{11}B and ^{13}C(d, α_1)^{11}B* are consistent with the results of Putt (1971) at higher deuteron energies.

1. Introduction

Nuclear transfer reaction studies utilising polarised and unpolarised beams provide useful information about nuclear structure, in particular about nuclear wavefunctions of few-nucleon systems (Brown *et al.* 1971; Das *et al.* 1992; Gomes *et al.* 1969; Knutson *et al.* 1973; Naqvi *et al.* 1992; Putt 1971; Sen and Knutson 1982; Yule and Haeberli 1968). The two-nucleon transfer (d, α) reaction cross section data are particularly useful for studying proton-hole and neutron-hole states in reactions on closed-shell nuclei (Gomes *et al.* 1969). Since the nuclear interior contributes substantially to the (d, α) reaction, it is necessary to take finite-range and non-locality corrections into account in DWBA model calculations. The simplest non-spherical relative motion in the α-particle is a D-state motion between two-deuteron clusters (d-d). D-state effects in the α-particles are very sensitive to the short-range behaviour of the nucleon–nucleon tensor force because the two deuterons must be in close proximity in order to be tightly bound in the α-particle. The analysing power A_{xx} of the (d, α) reaction is very sensitive to D-state contributions in the α-particle wavefunction and therefore the A_{xx} of (d, α) reaction data can be used to test realistic α-particle wavefunctions (Crosson *et al.* 1992). The cross section and tensor analysing power data of (d, α) cross sections are also used to calculate two-nucleon spectroscopic amplitudes

0004-9506/98/060903$05.00

and L-mixing ratios for unnatural-parity transition data (Crosson *et al.* 1993). The α-particle wavefunctions are further used in calculating the electromagnetic form factors, structure functions and spectra of present electronuclear (*e, enp*) studies (Schiavilla 1990; Schiavilla *et al.* 1990).

A program has been initiated at the Center for Applied Physical Sciences (CAPS) in which nuclear transfer reactions will be studied using polarised and unpolarised beams. The excitation functions and angular distribution of the ^{12}C(d, p) reaction were measured (Naqvi *et al.* 1992) as part of this program. Cross sections of the ^{13}C(d, α_0)^{11}B and ^{13}C(d, α_1)^{11}B* reactions have now been measured for deuteron energies in the 180–350 keV range. The main reason for choosing this reaction was the poor agreement between previously measured two-nucleon pickup ^{13}C(d, $\alpha_{0,1}$)^{11}B cross section data at 410–810 keV deuteron energies and DWBA calculations (Putt 1971). The calculations had underestimated the reaction cross section by several orders of magnitude and did not reproduce the shape of the experimental angular distributions of these reactions. The main reason for this disagreement was the limitation of the DWBA calculations to the zero-range approximation. Meanwhile the DWBA model calculations have been improved and the DWBA codes TWOFNR (Crosson *et al.* 1992, 1993) and PTOLEMY (Kozlowska *et al.* 1994) have been successfully used to calculate cross sections and analysing powers of transfer reactions after taking into consideration the finite-range approximation, multisteps in nuclear reactions and D-state effects in few-nucleon systems. Therefore it was worthwhile to measure cross section data for the ^{13}C(d, α_0)^{11}B and ^{13}C(d, α_1)^{11}B* reactions for comparison with improved DWBA calculations. Results of ^{13}C(d, α_0)^{11}B and ^{13}C(d, α_1)^{11}B* reaction cross section measurements at 180–350 keV deuteron energies are presented in this paper.

2. Experimental

The cross sections of the ^{13}C(d, α_0)^{11}B and ^{13}C(d, α_1)^{11}B* reactions were measured in the scattering chamber of the 80° beam line (Al-Jalal *et al.* 1995) of the CAPS 350 keV accelerator (Al-Juwair *et al.* 1987). Prior to the measurements, the beam energy of the 350 keV accelerator was calibrated using the 224 and 340 keV resonances of the ^{19}F(p, $\alpha\gamma$)^{16}O nuclear reaction. The cross section measurements were carried out using the procedure described earlier (Naqvi *et al.* 1992). The measurements were carried out using 8 silicon surface barrier detectors with 300 μm thickness and 100 mm^2 effective area. In this study 30 μg/cm^2 thick enriched ^{13}C foils were used as targets. The ^{13}C foils were supplied by Atomic Energy of Canada Ltd, Chalk River, Canada. The cross section data were acquired by the XSYS-based data acquisition and analysis facility of the CAPS (Al-Juwair and Abdel Aal 1989). The data acquisition facility, which was originally based around a VAX 11/785 computer, has been moved to a μ-VAX workstation. New hardware and software has been added to the facility so that one can acquire data from a maximum of 16 detectors simultaneously using one MBD channel.

The cross section of the ^{13}C(d, α_0)^{11}B reaction was measured between 180 and 350 keV, while that of the ^{13}C(d, α_1)^{11}B* reaction was measured between 250 and 350 keV. The excitation functions for both reactions were measured at 90° at an energy interval of 10 keV; angular distributions were measured at 14

angles between 30° and 164° in 10° steps. The angular distribution of the $^{13}C(d, \alpha_0)^{11}B$ reaction was measured at nine energies, namely 180, 200, 220, 250, 270, 290, 310, 335 and 350 keV, while those of the $^{13}C(d, \alpha_1)^{11}B^*$ reaction were measured at the six energies 250, 270, 290, 310, 335 and 350 keV. Fig. 1 shows a typical pulse height spectrum exhibiting proton, triton and α-particle peaks from $^{13}C(d, p)$, $^{13}C(d, t)$, $^{13}C(d, \alpha_0)$ and $^{13}C(d, \alpha_1)$ reactions. At all angles the α-particle peaks from the $^{13}C(d, \alpha_{0,1})$ reactions are totally resolved.

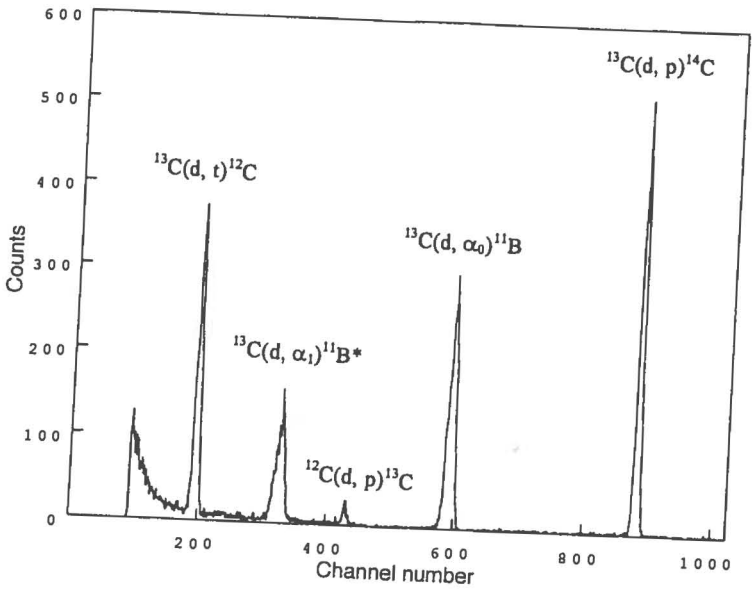

Fig. 1. A typical pulse height spectrum, showing proton, triton and α-particle peaks from $^{13}C(d, p)$, $^{13}C(d, t)$, $^{13}C(d, \alpha_0)$ and $^{13}C(d, \alpha_1)$ reactions at 30° for 335 keV deuterons.

The statistical uncertainties in the excitation functions and angular distribution of the $^{13}C(d, \alpha_0)^{11}B$ reaction were 2–10% and 2–24% respectively. The statistical uncertainties in the excitation functions and angular distribution of the $^{13}C(d, \alpha_1)^{11}B^*$ reaction were 5–6% and 2–8% respectively. The systematic uncertainties in cross section data, which were due to charge integration, target thickness and the finite angular resolution, were estimated to be 4–5%.

3. Results and Discussion

(3a) Excitation Function and Angular Distributions of the $^{13}C(d, \alpha_0)^{11}B$ Reaction

The excitation function of the $^{13}C(d, \alpha_0)^{11}B$ reaction at 90°, as shown in Fig. 2, has a structureless shape, with the cross section increasing smoothly with energy. The cross section has three regions with different slopes (rates of increase of cross section with energy). Above 280 keV energy the cross section slope is larger than that over the 230–280 keV range. Below 230 keV the cross section slope has its smallest value. The angular distributions of the $^{13}C(d, \alpha_0)^{11}B$ reaction for deuteron energies of 270–350 keV are shown in Fig. 3*a*, along with Legendre polynomial fits to the angular distribution data (plotted as solid curves). The angular distributions are asymmetric and backward-peaked, with minimum

cross sections at around 80°. Over the 290–350 keV range they are almost equally spaced, confirming the value of the cross section slope obtained at 90°. The separation between the angular distributions at 290 and 270 keV is smaller than at higher energies. With decreasing energy the angular distribution becomes more asymmetric, indicating an increasing contribution of direct reaction. Fig. 3*b* shows the angular distribution of the $^{13}C(d, \alpha_0)^{11}B$ reaction for 180–270 keV deuteron energies, along with Legendre polynomial fits. From the different spacing of the angular distributions, we expect that below 220 keV the cross section has a different slope. The angular distribution becomes more asymmetric with decreasing energy. Fig. 3*c* shows the angular distribution of $^{13}C(d, \alpha_0)^{11}B$ for 180–220 keV deuteron energies on an enlarged scale. The backward-peaking trend of the angular distributions in Fig. 3*c* clearly indicates a dominant contribution from the direct reaction channel over this energy range.

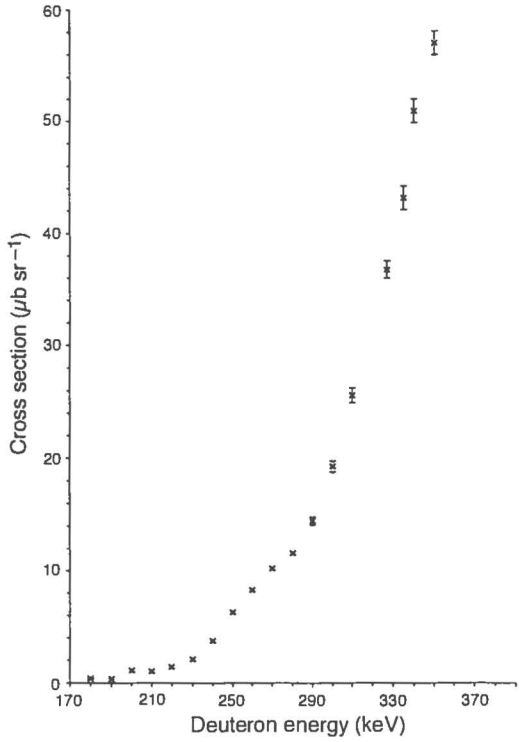

Fig. 2. Excitation function of the $^{13}C(d, \alpha_0)^{11}B$ reaction at 90°.

Comparison of the angular distribution data for the $^{13}C(d, \alpha_0)^{11}B$ reaction at 180–350 keV with those of Putt (1971) at 410–810 keV shows similar trends in the shape of angular distributions. Over the 410–810 keV deuteron energy range, Putt has also obtained a backward-peaked angular distribution for the $^{13}C(d, \alpha_0)^{11}B$ reaction, but the backward peaking we have observed is stronger. For our data, the cross section at forward angles decreased rapidly with energy compared to that at backward angles. For example, the cross section at 165° has decreased by a factor of 107 for a decrease in deuteron energy from 350 to

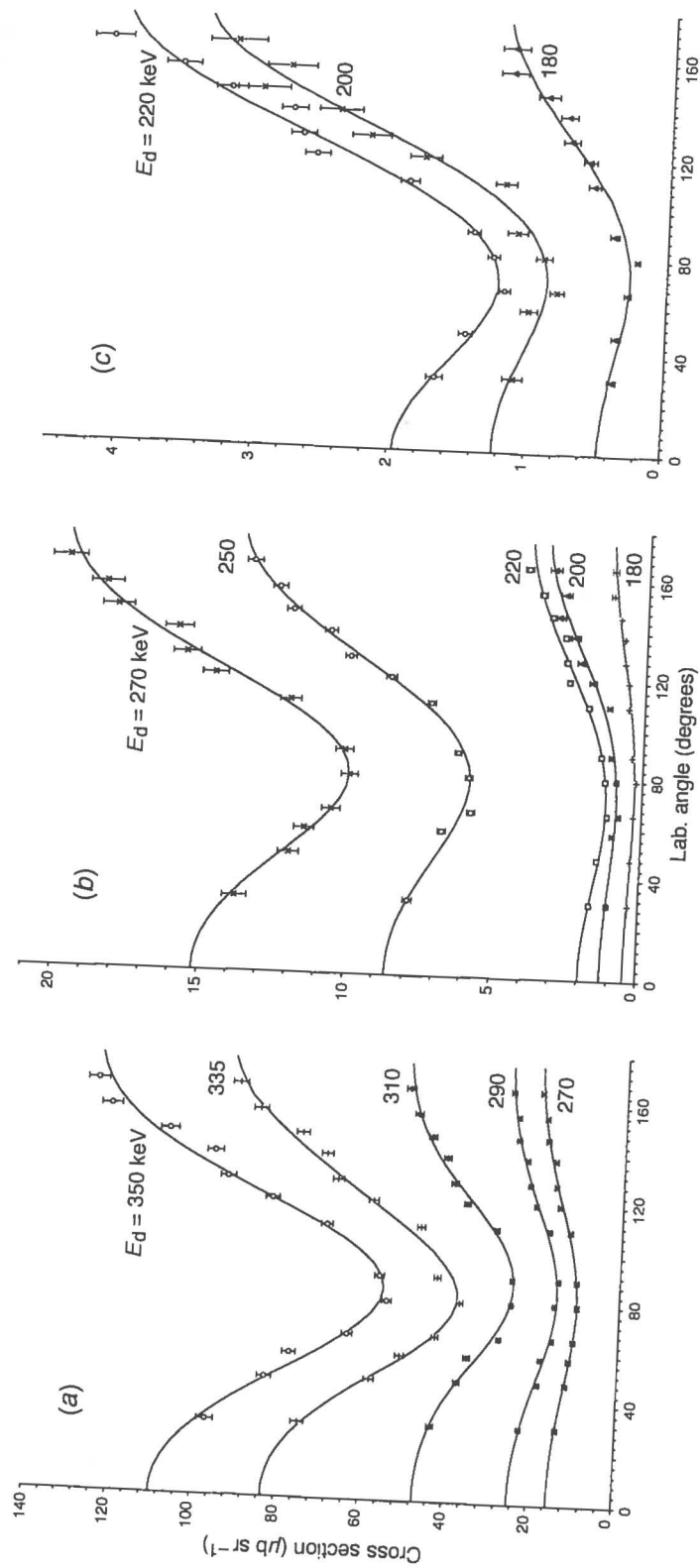

Fig. 3. Angular distributions of the $^{13}C(d, \alpha_0)^{11}B$ reaction for: (*a*) 270, 290, 310, 335 and 350 keV deuterons; (*b*) 180, 200, 220, 250 and 270 keV deuterons; and (*c*) 180, 200 and 220 keV deuterons. The curves are Legendre polynomial fits.

180 keV. Over the same energy range, the cross section at 30° has decreased by a factor of 250, indicating strong backward peaking of the angular distribution at very low deuteron energies in the present work. This shows increasing direct reaction contributions with decreasing deuteron energy in the $^{13}C(d, \alpha_0)^{11}B$ reaction data obtained in the present study.

(3b) Excitation Function and Angular Distributions of the $^{13}C(d, \alpha_1)^{11}B^*$ Reaction

The excitation function of the $^{13}C(d, \alpha_1)^{11}B^*$ reaction at 90°, as shown in Fig. 4, does not show structure. It has two different cross section slopes, one above and the other below 280 keV deuteron energy. This difference in value of the cross section slope at 90° is demonstrated by the different spacings between the angular distributions of the $^{13}C(d, \alpha_0)^{11}B^*$ reaction at deuteron energies of 250–350 keV, as shown in Fig. 5. Legendre polynomial fits to the angular distribution data are also shown in Fig. 5. Within the statistical uncertainties, all of the distributions show a smooth trend and have no structure. The angular distributions are symmetric about 90°, indicating a dominating contribution from the compound nucleus reaction. With decreasing energy the angular distributions retain their symmetric shape.

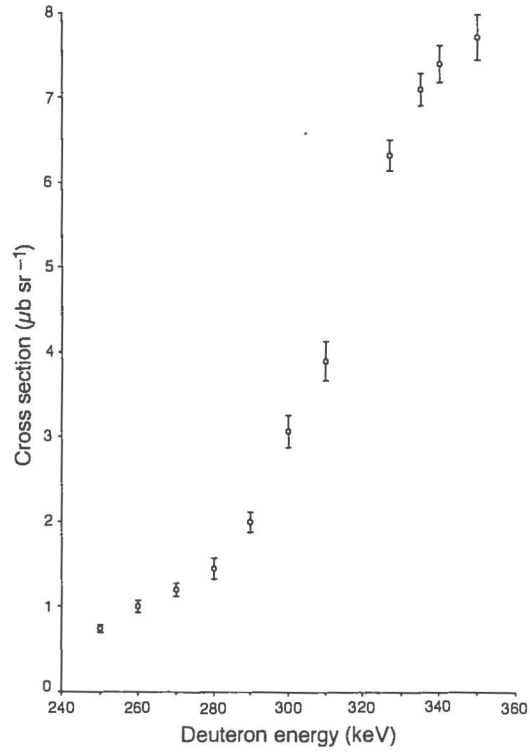

Fig. 4. Excitation function of the $^{13}C(d, \alpha_1)^{11}B^*$ reaction at 90°.

The symmetric shape of the angular distributions is in agreement with trends in the angular distribution data for the $^{13}C(d, \alpha_1)^{11}B^*$ reaction at 410–810 keV deuteron energies measured by Putt (1971). For 510–810 keV deuteron energies,

Putt measured forward-peaked angular distributions. At 410 keV deuteron energy the cross section increases suddenly at backward angles, and the angular distribution is almost symmetric in shape. This trend has continued at the lower energies covered in the present study, and we have measured symmetric angular distributions for the $^{13}C(d, \alpha_1)^{11}B^*$ reaction in this study. In spite of the symmetric shape, all of these angular distributions have the steep slopes that are characteristic of non-compound nucleus reactions.

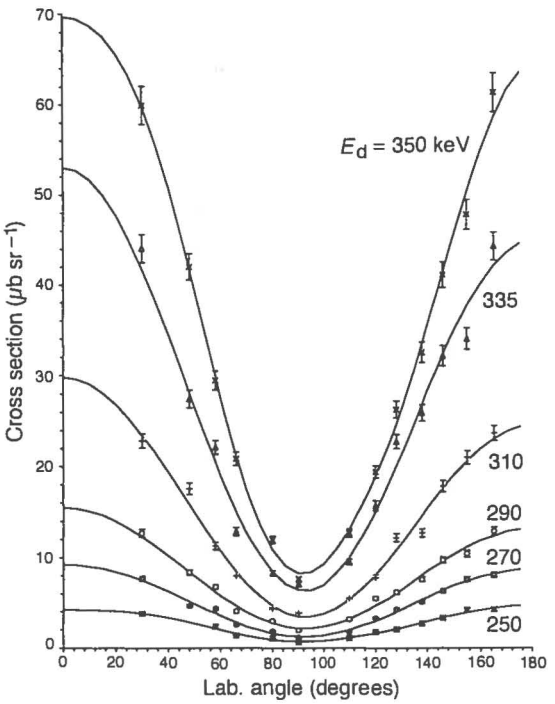

Fig. 5. Angular distributions of the $^{13}C(d, \alpha_1)^{11}B^*$ reaction for 250, 270, 290, 310, 335 and 350 keV deuterons, together with Legendre polynomial fits (solid curves).

Table 1. Total cross sections of the $^{13}C(d, \alpha_0)^{11}B$ and $^{13}C(d, \alpha_1)^{11}B^*$ reactions (in μb)

Deuteron lab. energy (keV)	$^{13}C(d, \alpha_0)^{11}B$	$^{13}C(d, \alpha_1)^{11}B^*$
180	6±2·5	—
200	18±4	—
220	24±4	—
250	99±11	27±6
270	162±14	49±7
290	240±17	79±9
310	441±23	143±12
335	722±29	259±16
350	1009±34	353±20

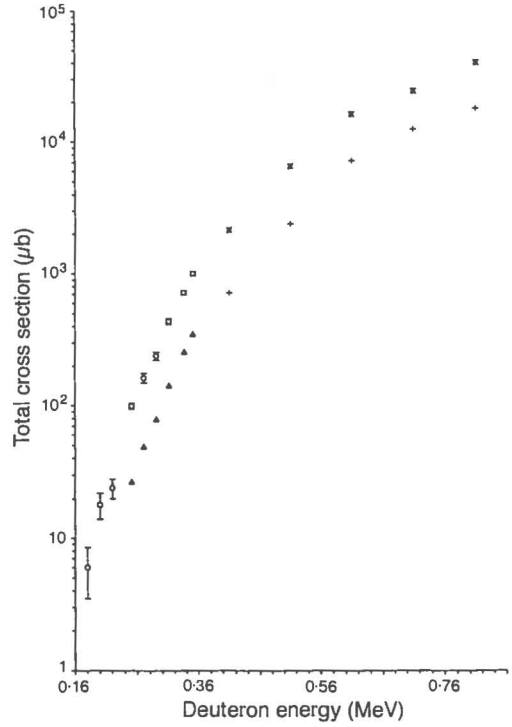

Fig. 6. Total cross sections of the $^{13}C(d, \alpha_0)^{11}B$ and $^{13}C(d, \alpha_1)^{11}B^*$ reactions for 180–350 keV deuterons (circles and triangles), together with the data of Putt (1971) (crosses and pluses).

(3c) Total Cross Sections of the $^{13}C(d, \alpha_0)^{11}B$ and $^{13}C(d, \alpha_1)^{11}B$ Reactions

The experimental total cross sections of the $^{13}C(d, \alpha_0)^{11}B$ and $^{13}C(d, \alpha_1)^{11}B^*$ reactions, which were calculated from the Legendre polynomial fits to the angular distribution data, are listed in Table 1. Also given are the uncertainties in total cross section, which were calculated from the uncertainty in a_0, i.e. the $l = 0$ term of the Legendre polynomial fit. Fig. 6 shows the total cross sections of the $^{13}C(d, \alpha_0)^{11}B$ and $^{13}C(d, \alpha_1)^{11}B^*$ reactions as functions of deuteron energy. For the sake of comparison, experimental total cross section data for the $^{13}C(d, \alpha_0)^{11}B$ and $^{13}C(d, \alpha_1)^{11}B^*$ reactions at 410–810 keV, taken from Putt (1971), are also plotted in Fig. 6. The cross section data measured in the present study follow the smooth trend of Putt's data.

Acknowledgment

This work is part of a research project at the Center for Applied Physical Sciences of King Fahd University of Petroleum and Minerals, Dhahran, Saudi Arabia.

References

Al-Jalal, A. M., Naqvi, A. A., Al-Juwair, H. A., Coban, A., and Khiari, F. Z. (1995). *Arab. J. Sci. Eng.* **20**, 179.

Al-Juwair, H., and Abdel Aal, R. E. (1989). *IEEE Trans. Nucl. Sci.* **NS-36**, 611.
Al-Juwair, H., Blume, G., Jarasma, R. J., Meitzler, C. R., and Purser, K. H. (1987). *Nucl. Instrum. Meth.* B **24/25**, 810.
Brown, R. C., Debenham, A. A., Greenlees, G. W., Griffith, J. A. R., Karban, O., Kocher, D. C., and Roman, S. (1971). *Phys. Rev. Lett.* **27**, 1446.
Crosson, E. R., Das, R. K., Lemieux, S. K., Ludwig, E. J., Thompson, W. J., Bisenberger, M., Hertenberger, R., Hofer, D., Kader, H., Schiemenz, P., Graw, G., Eiro, A. M., and Santos, F. D. (1992). *Phys. Rev.* C **45**, R492.
Crosson, E. R., Ludwig, E. J., Bisenberger, M., Hertenberger, R., Hofer, D., Kader, H., Schiemenz, P., Graw, G., Eiro, A. M., Santos, F. D., and Brown, B. A. (1993). *Phys. Rev.* C **48**, 1770.
Das, R. K., Clegg, T. B., Karwowski, H. J., and Ludwig, E. J. (1992). *Phys. Rev. Lett.* **68**, 1112.
Gomes, P. V., Ueta, N., Douglas, R. A., Sala, O., Wildmore, D., Robson, B. A., and Hodgson, P. E. (1969). *Nucl. Phys.* A **136**, 385.
Knutson, L. D., Stephenson, E. J., Rohrig, N., and Haeberli, W. (1973). *Phys. Rev. Lett.* **31**, 392.
Kozlowska, B., Ayer, Z., Das, R. K., Karwowski, H. J., and Ludwig, E. J. (1994). *Phys. Rev.* C **50**, 2695.
Naqvi, A. A., Al-Jalal, M. A., Coban, A., and Khiari, F. Z. (1992). *Nuovo Cimento* A **105**, 1501.
Putt, G. D. (1971). *Nucl. Phys.* A **161**, 547.
Schiavilla, R. (1990). *Phys. Rev. Lett.* **65**, 835.
Schiavilla, R., Pandharipande, V. R., and Riska, D. O. (1990). *Phys. Rev.* C **41**, 309.
Sen, S., and Knutson, L. D. (1982). *Phys. Rev.* C **26**, 257.
Yule, T. J., and Haeberli, W. (1968). *Nucl. Phys.* A **117**, 1.

Manuscript received 8 April, accepted 3 July 1998